Mössbauer Study of *D. gigas* Ferredoxin II and Spin-Coupling Model for the Fe_3S_4 Cluster with Valence Delocalization

V. Papaefthymiou,[†] J.-J. Girerd,[‡] I. Moura,[§] J. J. G. Moura,[§] and E. Münck*[†]

Contribution from the Gray Freshwater Biological Institute, University of Minnesota, Navarre, Minnesota 55392, Laboratoire de Spectrochimie des Elements de Transition, Equipe de Recherche Associee au CNRS, No. 672, Universite de Paris-Sud, 91405 Orsay, France, and Centro de Quimica Estrutural, UNL 1000 Lisboa, Portugal. *Received December 22, 1986*

Abstract: The electron transport protein ferredoxin II (Fd II) from *Desulfovibrio gigas* contains an iron-sulfur cluster with an Fe_3S_4 core. We have studied the protein in the reduced state (cluster spin $S = 2$) with Mössbauer spectroscopy between 1.3 and 210 K in magnetic fields up to 6.0 T. Below 20 K one iron site of the cluster is Fe^{3+} whereas the other two sites form a delocalized Fe^{2+}/Fe^{3+} pair. The itinerant electron is evenly delocalized over the pair. X-band EPR at 9 K reveals a "$\Delta m = 4$" transition between two levels of the spin quintet. The highly resolved Mössbauer spectra were analyzed with an $S = 2$ spin Hamiltonian; 16 electronic and hyperfine parameters were determined with good precision. The positive magnetic hyperfine coupling constant $A_{II} = +15.6$ MHz of the Fe^{3+} site shows that its local spin is antiparallel coupled to the system spin, and its magnitude suggests a spin of $^9/_2$ for the delocalized dimer. The data were analyzed with a spin coupling model which takes into account Heisenberg exchange and valence delocalization. The description of the latter is gleaned from the Anderson-Hasegawa theory of double exchange. The effective Hamiltonian proposed here describes the data very well, and it holds promise for the description of valence-delocalized clusters with Fe_4S_4 cores. Above 20 K an additional spectral component appears in the Mössbauer spectra, suggesting population of an excited state with electron delocalization over all three sites. The transition rate between the ground-state and excited-state configuration is slow on the Mössbauer time scale ($\sim 10^{-7}$ s). Such a situation has not yet been reported for any iron-sulfur cluster.

Ferredoxin II (Fd II) from *Desulfovibrio gigas* is an electron-transfer protein with a variety of interesting properties. The protein is a tetramer consisting of identical subunits of known sequence, each having a molecular mass of 6000 dalton.[1] Each subunit contains a trinuclear iron-sulfur cluster,[2] presumably of the Fe_3S_4 type.[3,4] Although high-resolution X-ray crystallographic data are not available, spectroscopic and chemical data suggest a cubane structure such as those observed for Fe_4S_4 clusters, with one iron site unoccupied. This is supported by an average Fe-Fe distance of 2.7 Å (typical for cubanes) which has been deduced from extended X-ray absorption fine structure studies.[4] Furthermore, cluster conversion experiments[5] have demonstrated the formation of a cluster with an Fe_4S_4 core when the protein is incubated with ferrous ion. More recently, the Fe_3S_4 cluster of Fe(II) has been used as a precursor for the formation of a $CoFe_3S_4$ cluster.[6]

In the past few years, we have studied Fd II extensively with Mössbauer and EPR spectroscopy. These studies have shown that the clusters of the four subunits are equivalent and magnetically noninteracting. Thus, for the present paper, we can consider Fd II as a protein of molecular mass 6000 dalton containing *one* Fe_3S_4 cluster.

The Mössbauer spectroscopic data of Fd II are very similar to those reported for other proteins containing trinuclear clusters such as aconitase,[7] a ferredoxin from *A. vinelandii*,[8] *Desulfovibrio gigas* hydrogenase,[9] and a ferredoxin from *Thermus thermophilus*.[10] With the exception of beef heart aconitase (which is difficult to obtain enriched in ^{57}Fe), all other proteins contain at least one other type of iron-sulfur cluster in addition to the trinuclear center. This leaves Fd II as the protein of choice for cluster conversion experiments and high-resolution Mössbauer studies.

The cluster of Fd II can be stabilized in two oxidation states. In the oxidized form the cluster has electronic spin $S = {}^1/_2$ which results from antiferromagnetic coupling of three high-spin ferric ($S_1 = S_2 = S_3 = {}^5/_2$) ions.[11] Mössbauer spectra taken at $T >$ 40 K (in the limit of fast electronic spin relaxation) exhibit *one* sharp quadrupole doublet (see Figure 1A) with quadrupole splitting, $\Delta E_Q = 0.53$ mm/s, and isomer shift, $\delta = 0.28$ mm/s. These parameters are typical for Fe^{3+} in a tetrahedral environment of thiolate ligands. At 4.2 K (slow relaxation) the Mössbauer spectra exhibit three distinct magnetic components.[2] The data have been analyzed[11] with a Heisenberg Hamiltonian which assumes isotropic antiferromagnetic coupling among three rubredoxin-type ferric sites.

Reduction by one electron, $E_m = -130$ mV (vs. NHE) yields a state with integer cluster spin. Preliminary Mössbauer studies[2] in weak applied fields have shown that the zero-field splitting parameters are such that the two lowest electronic states are separated in energy by about 0.35 cm^{-1}. Subsequently, Thomson and co-workers[12] have studied reduced Fd II with low-temperature magnetic circular dichroism and inferred that the ground manifold has $S = 2$.

The 4.2 K zero-field Mössbauer spectrum of the reduced cluster[2] exhibit two quadrupole doublets (see Figure 1B) with intensity ratio 2:1. The more intense doublet, representing two iron sites (we have referred[2] to both sites as site I), has ΔE_Q (I) = 1.47 mm/s and δ (I) = 0.46 mm/s. The second doublet (site II) has ΔE_Q (II) = 0.52 mm/s and δ (II) = 0.32 mm/s. The parameters of site II are essentially the same as those of the oxidized cluster.

[†] University of Minnesota.
[‡] Universite de Paris-Sud.
[§] Centro de Quimica Estrutural.

(1) Xavier, A. V.; Moura, J. J. G.; Moura, I. *Struct. Bonding* **1981**, *43*, 187-213.
(2) Huynh, B. H.; Moura, J. J. G.; Moura, I.; Kent, T. A.; LeGall, J.; Xavier, A. V.; Münck, E. *J. Biol. Chem.* **1980**, *255*, 3242-3244.
(3) Beinert, H.; Thomson, A. J. *Arch. Biochem. Biophys.* **1983**, *222*, 333-361.
(4) Antonio, M. R.; Averill, B. A.; Moura, I.; Moura, J. J. G.; Orme-Johnson, W. H.; Teo, B.-K.; Xavier, A. V. *J. Biol. Chem.* **1982**, *257*, 6646-6649.
(5) Moura, J. J. G.; Moura, I.; Kent, T. A.; Lipscomb, J. D.; Huynh, B. H.; LeGall, J.; Xavier, A. V.; Münck, E. *J. Biol. Chem.* **1982**, *257*, 6259-6267.
(6) Moura, I.; Moura, J. J. G.; Münck, E.; Papaefthymiou, V.; LeGall, J. *J. Am. Chem. Soc.* **1986**, *108*, 349-351.
(7) Kent, T. A.; Dreyer, J.-L.; Kennedy, M. C.; Huynh, B. H.; Emptage, M. H.; Beinert, H.; Münck, E. *Proc. Natl. Acad. Sci. U.S.A.* **1982**, *79*, 1096-1100.
(8) Emptage, M. H.; Kent, T. A.; Huynh, B. H.; Rawlings, J.; Orme-Johnson, W. H.; Münck, E. *J. Biol. Chem.* **1980**, *255*, 1793-1796.
(9) Huynh, B. H.; Czechowski, M. H.; Krüger, H.-J.; DerVartanian, D. V.; Peck, H. D.; LeGall, J. *Proc. Natl. Acad. Sci. U.S.A.* **1984**, *81*, 3728-3732.
(10) Hille, R.; Yoshida, T.; Tarr, G. E.; Williams, C. H.; Ludwig, M. L.; Fee, J. A.; Kent, T. A.; Huynh, B. H.; Münck, E. *J. Biol. Chem.* **1983**, *258*, 13008-13013.
(11) Kent, T. A.; Huynh, B. H.; Münck, E. *Proc. Natl. Acad. Sci. U.S.A.* **1980**, *77*, 6574-6576.
(12) Thomson, A. J.; Robinson, A. E.; Johnson, M. K.; Moura, J. J. G.; Moura, I.; Xavier, A. V.; LeGall, J. *Biochim. Biophys. Acta.* **1981**, *670*, 93-100.

0002-7863/87/1509-4703$01.50/0

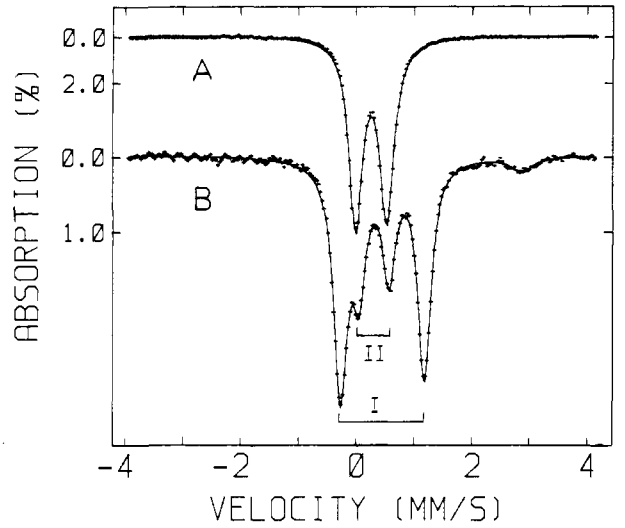

Figure 1. Mössbauer spectra of ^{57}Fe enriched Fd II: (A) oxidized sample at 100 K and (B) reduced sample at 4.2 K. Both spectra were recorded in zero magnetic field.

Thus, the iron of site II has remained high-spin Fe^{3+}. The parameters of site I, on the other hand, are just the average of those observed for oxidized and reduced tetrahedral sulfur sites,[13] suggesting that the electron that has entered the cluster upon reduction is shared equally by the two irons of site I. Thus, site I comprises two irons at the oxidation level Fe.[2.5+] This provides us with a mixed-valency system with one localized site (the Fe^{3+} of site II) and a delocalized pair. Since the reduced cluster is an integer spin paramagnet, the zero-field Mössbauer spectra exhibit quadrupole doublets only. In strong applied fields, however, Fd II yields well-resolved spectra exhibiting magnetic hyperfine structure. By analyzing these spectra, we have determined the zero-field splittings and a complete set of hyperfine parameters. These parameters allow us to elucidate the coupling mechanism of the reduced Fe_3S_4 cluster.

From a standpoint of mixed valency the simple iron–sulfur clusters which have been studied in proteins can roughly be divided into localized and delocalized systems.[14] Reduced clusters with a $[Fe_2S_2]^{1+}$ core such as observed in spinach ferredoxin,[15] putidaredoxin,[16] or the Rieske protein[17] have clearly recognizable localized Fe^{3+} and Fe^{2+} sites. The superexchange coupling between the two sites is well described by the Heisenberg Hamiltonian $\mathcal{H} = J\vec{S}_1\cdot\vec{S}_2$. This is of benefit for structural studies because the coupling model allows one to deduce the g values and the magnetic hyperfine tensors of the uncoupled sites from those of the (observed) coupled sites. Indeed, the correct structure of the Fe_2S_2 clusters was deduced from spectroscopic studies before the X-ray structure became available. In contrast to Fe_2S_2 clusters, the $[Fe_4S_4]^{3+}$ and $[Fe_4S_4]^{1+}$ cubanes are delocalized mixed-valence systems for which a suitable coupling model has not emerged. The Heisenberg Hamiltonian is inadequate because electron delocalization produces a coupling mechanism completely different from the usual superexchange of localized systems. The problem of delocalization of an excess electron was first considered by Zener[18] and Anderson and Hasegawa[19] in their fundamental papers on "double-exchange". Recently, Noodleman and Baerends[20] have discussed this problem in the framework of LCAO-Xα valence bond theory. These authors have pointed out that the delocalization favors a parallel spin alignment of the valence electrons. If superexchange and delocalization are taken into account, the energy levels of a mixed-valence dimer are given by[20,21] $E(S) = {}^{J}/_{2}S(S+1) \pm B(S+{}^{1}/_{2})$, where J is the usual superexchange coupling constant and B the matrix element responsible for the transfer of the excess electron. Thus, the system is not describable by the Heisenberg Hamiltonian $\mathcal{H} = J\vec{S}_1\cdot\vec{S}_2$. Although B is expected to be large, most dimer systems display localized valences. Various authors[22,23] have pointed out that vibronic coupling may reduce the B term.

Fe_3S_4 clusters exhibit both localized and delocalized valence states. Successful coupling models using the Heisenberg Hamiltonian have been published for the oxidized ($S = {}^{1}/_{2}$) 3-Fe clusters[11] and for the linear ($S = {}^{5}/_{2}$) Fe_3S_4 structures.[24,25] In both systems, all iron sites are high-spin Fe^{3+}. As pointed out above the cluster of reduced Fd II has a localized site and a delocalized pair. Münck and Kent[26] have argued that the spin of the internally delocalized dimer is $S = {}^{9}/_{2}$, suggesting a parallel alignment of the valence electrons and thus a double-exchange-type mechanism.

In this paper, we present a series of high-field Mössbauer spectra and discuss their analysis by means of a spin Hamiltonian. In the subsequent theoretical section, we introduce a Hamiltonian which takes superexchange and electron delocalization into account.

Materials and Methods

Ferredoxin II was purified as described previously.[2,27] The Mössbauer spectrometer and data reduction methods have been described elsewhere.[14a] All isomer shifts are quoted relative to Fe metal at room temperature. EPR spectra were recorded on a Varian E-109 spectrometer fitted with an Oxford Instruments ESR-10 continuous flow helium cryostat.

(13) Rubredoxin is the prototype of mononuclear Fe^{3+} or Fe^{2+} sites with a tetrahedral cysteine–sulfur environment. The protein from *Clostridium pasteuranium* has been studied in great detail with Mössbauer spectroscopy. (a) Schulz, C.; Debrunner, P. G. *J. Physique* (Supplement 12) **1976**, *37*, 153–158. Oxidized rubredoxin ($S = {}^{5}/_{2}$) has $\Delta E_Q = -0.50$ mm/s and $\delta = 0.32$ mm/s whereas the reduced protein site ($S = 2$) exhibits $\Delta E_Q = -3.25$ mm/s and $\delta = 0.70$ mm/s (all parameters at 4.2 K). Similiar parameters have been reported for synthetic analogues for the active site of rubredoxin. (b) Winkler, H.; Kostikas, A.; Petrouleas, V.; Simopoulos, A.; Trautwein, X. A. *Hyperfine Interact.* **1986**, *29*, 1347–1350. Desulforedoxin from *D. gigas* is another protein with tetrahedral-type sulfur ligation: (c) Moura, I.; Huynh, B. H.; Hausinger, R. P.; LeGall, J.; Xavier, A. V.; Münck, E. *J. Biol. Chem.* **1980**, *255*, 2493–2498. This protein has $\Delta E_Q = -0.75$ mm/s and $\delta = 0.25$ mm/s in the Fe^{3+} state and $\Delta E_Q = +3.55$ mm/s and $\delta = 0.70$ mm/s in the Fe^{2+} state. The main difference between rubredoxin and desulforedoxin is the sign of ΔE_Q for the reduced states. Thus, the former has mainly an orbital ground state with d_{z^2} symmetry whereas the latter has an orbital with predominant $d_{x^2-y^2}$ character.

(14) An exception appear to be the P-clusters of nitrogenase which exhibit one localized (component Fe^{2+}) and three delocalized sites (component D). Although the evidence favors a cubane Fe_4S_4 core, X-ray crystallographic data for these spectroscopically unique clusters have not yet reported: (a) Zimmermann, R.; Münck, E.; Brill, W. J.; Shah, V. K.; Henzl, M. T.; Rawlings, J.; Orme-Johnson, W. H. *Biochim. Biophys. Acta* **1978**, *537*, 185–207. A localized valence has been observed for the Fe_4S_4 cluster of aconitase upon binding of substrates and inhibitors. (b) Emptage, M. H.; Kent, T. A.; Kennedy, M. C.; Beinert, H.; Münck, E. *Proc. Natl. Acad. Sci. U.S.A.* **1983**, *80*, 4674–4678.

(15) (a) Dunham, W. R.; Palmer, G.; Sands, R. H.; Bearden, A. J. *Biochim. Biophys. Acta* **1971**, *253*, 373–384. (b) Sands, R. H.; Dunham, W. R. *Quart. Rev. Biophys.* **1975**, *7*, 443–504.

(16) Münck, E.; Debrunner, P. G.; Tsibris, J. C. M.; Gunsalus, I. C. *Biochemistry* **1971**, *11*, 855–863.

(17) Fee, J. A.; Findling, K. L.; Yoshida, T.; Hille, R.; Tarr, G. E.; Hearshen, D. O.; Dunham, W. R.; Day, E. P.; Kent, T. A.; Münck, E. *J. Biol. Chem.* **1984**, *259*, 124–133.

(18) Zener, C. *Phys. Rev.* **1951**, *82*, 403–405.

(19) Anderson, P. W.; Hasegawa, H. *Phys. Rev.* **1955**, *100*, 675–681.

(20) Noodleman, L.; Baerends, E. J. *J. Am. Chem. Soc.* **1984**, *106*, 2316–2327.

(21) Borshch, S. A.; Kotov, I. N.; Bersuker, I. B. *Sov. J. Chem. Phys.* **1985**, *3*, 1009–1016. Borshch, S. A. *Sov. Phys. Solid. State* **1984**, *26*, 1142–1143.

(22) Delocalized mixed valence systems have recently been discussed by the following: (a) Girerd, J.-J. *J. Chem. Phys.* **1983**, *79*, 1766–1775. (b) Belinskii, M. I.; Tsukerblat, B. S.; Gerbeleu, N. V. *Sov. Phys. Solid State* **1983**, *26*, 1142–1145. (c) Pourroy, G.; Coronado, E.; Drillon, M.; Georges, R. *Chem. Phys.* **1986**, *104*, 73–81.

(23) See, also: *Mixed Valence Compounds, Theory and Applications in Chemistry, Physics, Geology, and Biology*; Brown, D. B., Ed.; Reidel: Boston, 1980.

(24) Kennedy, M. C.; Kent, T. A.; Emptage, M.; Merkle, H.; Beinert, H.; Münck, E. *J. Biol. Chem.* **1984**, *259*, 14463–14471.

(25) Girerd, J.-J.; Papaefthymiou, G. C.; Watson, A. D.; Gamp, E.; Hagen, K. S.; Edelstein, N.; Frankel, R. B.; Holm, R. H. *J. Am. Chem. Soc.* **1984**, *106*, 5941–5947.

(26) Münck, E.; Kent, T. A. *Hyp. Int.* **1986**, *27*, 161–172.

(27) Bruschi, M.; Hatchikian, E. C.; LeGall, J.; Moura, J. J. G.; Xavier, A. V. *Biochim. Biophys. Acta.* **1976**, *449*, 275–284.

Table I. Hyperfine Parameters of Reduced Ferredoxin II[b]

	δ (mm/s)	ΔE_Q (mm/s)	η	β	A_x (MHz)	A_y (MHz)	A_z (MHz)	A_{av} (MHz)	A_{theory} (MHz)
site I	0.46 (1)	1.47 (2)	0.4 (2)	20 (5)	-20.5 (10)	-20.5 (10)	-16.4 (5)	-19.1	$A_A = A_B = -19.2$
site II	0.32 (1)	-0.52 (1)[a]	-2.0 (2)[a]	16 (5)	+13.7 (10)	+15.8 (10)	+17.3 (5)	+15.6	$A_C = +16.7$

[a] In a coordinate frame where $|V_{\xi\xi}| \geq |V_{\eta\eta}| \geq |V_{\zeta\zeta}|$ these parameters are $\Delta E_Q = +0.52$ mm/s and $\eta = 0.33$. [b] The zero-field splitting parameters were determined to be $D = -(2.5 \pm 0.5)$ cm^{-1} and $E/D = 0.23 \pm 0.02$. β is the polar angle between the z axes of zero-field splitting and EFG tensors. The numbers in parantheses give the estimated uncertainties of the least significant digits. In the last column are listed the theoretical values for sites I and II.

Results

Low-Temperature Spectra. A zero-field Mössbauer spectrum of reduced Fd II is shown in Figure 1B. The 4.2 K spectrum is dominated by the two quadrupole doublets of site I (two Fe) and site II (1 Fe). The ^{57}Fe-enriched sample studied here contained an Fe^{2+} impurity ($\Delta E_Q \approx 3.05$ mm/s and $\delta \approx 1.35$ mm/s) which accounts for about 7% of the total Fe in the sample. The high-energy line of this impurity is indicated by the shallow peak at +2.9 mm/s Doppler velocity. In the following, we will ignore the impurity[28] since its presence will practically not affect the analysis of the low-temperature spectra.

Figures 2 and 3 show spectra obtained by studying the sample in strong applied fields in the temperature range from 1.3 to 9.5 K. They exhibit richly structured hyperfine patterns from which a wealth of information can be extracted. We have analyzed these spectra in the framework of the $S = 2$ spin Hamiltonian. D and

$$\hat{\mathcal{H}} = \hat{\mathcal{H}}_e + \hat{\mathcal{H}}_{hf} \quad (1)$$

$$\text{with } \hat{\mathcal{H}}_e = D\left[S_z^2 - \frac{1}{3}S(S+1) + \frac{E}{D}(S_x^2 - S_y^2)\right] + 2\beta\vec{S}\cdot\vec{H} \quad (2)$$

$$\hat{\mathcal{H}}_{hf} = \sum_{i=I,II}[\vec{S}\cdot\tilde{A}(i)\cdot\vec{I}(i) - g_n\beta_n\vec{H}\cdot\vec{I}(i) + \hat{\mathcal{H}}_Q(i)] \quad (3)$$

$$\hat{\mathcal{H}}_Q = \frac{eQV_{\zeta\zeta}}{12}[3I_\zeta^2 - I(I+1) + \eta(I_\xi^2 - I_\eta^2)] \quad (4)$$

E are the zero-field splitting parameter. The Zeeman term is assumed to be isotropic, with $g = 2$. This is a good approximation because the g values of a rubredoxin-type Fe^{2+} site deviate by less than 10% from $g = 2$. Thus for a cluster which comprises formally two ferric ions ($g = 2$) and one ferrous ion we expect small deviations from $g = 2$. In eq 3 the magnetic hyperfine interactions, the nuclear Zeeman term, and the quadrupole interactions are added for the two distinguishable sites, i = I and II. We have found that the electric field gradient (EFG) tensors are rotated relative to the frame (x, y, z) defined by the zero-field splitting tensors. In eq 4, we have expressed $\mathcal{H}_Q$ in its standard principal axis form.

We have performed extensive spectral simulations with use of computer programs and equipment described previously.[14a] The solid lines in Figures 2 and 3 are theoretical curves based on eq 1–4 with use of the parameter set listed in Table I. In the following, we discuss how these parameters were determined.

1. As reported earlier the 4.2 K spectrum of Fd II exhibits already sizeable but poorly resolved hyperfine interactions (see Figure 7B of ref 29) in an applied field of 0.06 T. From this observation, two important conclusions can be drawn. Since an applied field of 0.06 T induces a sizeable hyperfine field, $H_{int} \approx$ 12 T, two sublevels of the spin quintet must be separated in energy

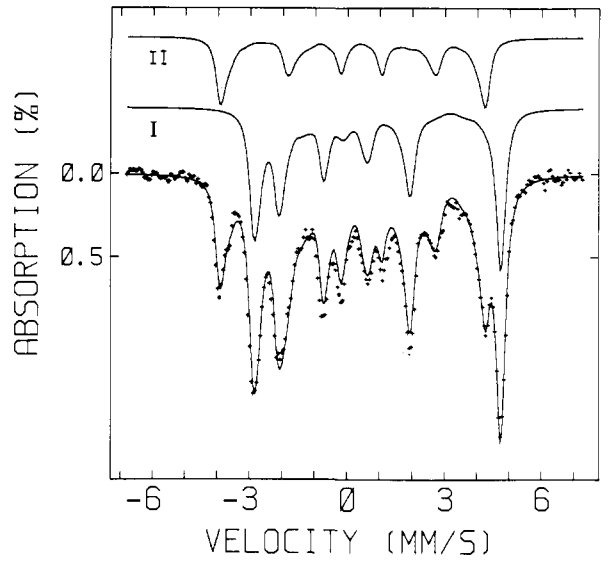

Figure 2. Mössbauer spectrum of reduced Fd II taken at 1.3 K in a field of 1.0 T applied parallel to the γ-beam. The solid line drawn through the data is a spectral simulation with the parameters of Table I. Above the data are shown the individual spectra of sites I (two iron atoms) and II.

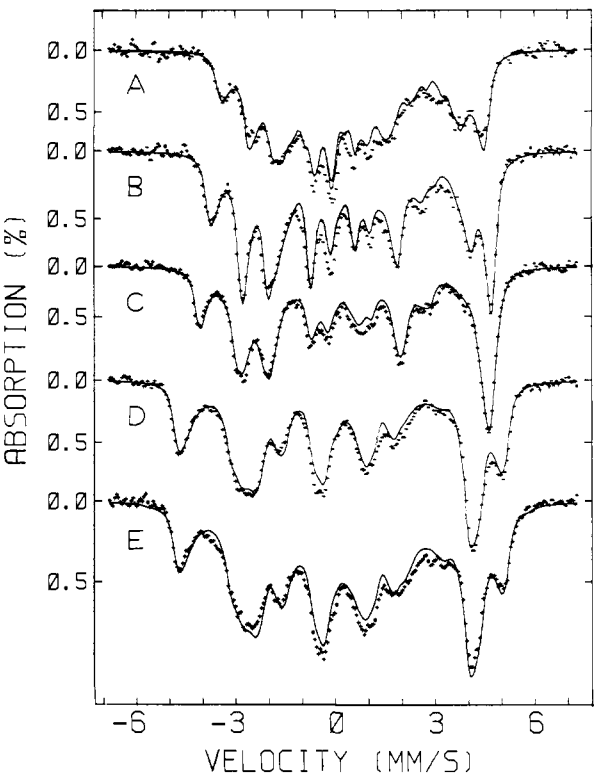

Figure 3. Low-temperature Mössbauer spectra of reduced ^{57}Fe enriched Fd II. The solid lines are theoretical curves computed with the parameters of Table I. The theoretical spectra are normalized to represent 93% of the total absorption; the Fe^{2+} impurity is not considered. Spectra (A)–(D) were recorded at 4.2 K, spectrum (E) at 9.5 K. The parallel applied fields were (A) 0.25, (B) 0.5, (C) 2.0, (D) 6.0, and (E) 6.0 T.

(28) The impurity is almost certainly the result of cluster destruction caused by reducing the sample with dithionite. The oxidized material was free of any discernible impurity. The presence of the 7% impurity affects the fitting of the high-temperature spectra. For the high-temperature spectra we have therefore studied a sample, containing ^{57}Fe in natural abundance, which was free of impurities. The Mössbauer spectra of this sample are shown in Figure 6 and its X-band EPR spectrum is displayed in Figure 5. There is a small difference between the spectra of the enriched sample and the natural abundance sample: the latter has ΔE_Q (I) = 0.47 mm/s rather than ΔE_Q (I) = 0.52 mm/s at 4.2 K. All other parameter are the same within the uncertainties.

(29) Münck, E. In *Mössbauer Spectroscopy and Its Chemical Applications*; Stevens, J. G., Shenoy, G. K., Eds.; American Chemical Society: Washington, DC, 1981; pp 305–328.

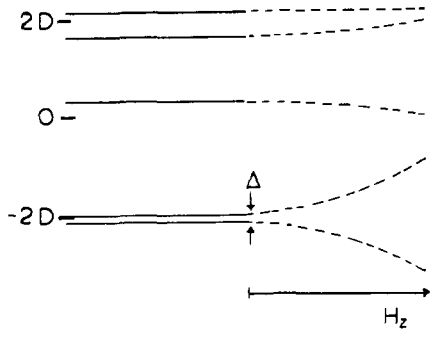

Figure 4. Energy level diagram for $S = 2$ manifold for $D = -2.5$ cm^{-1} and $E/D = 0.23$. Dashed lines indicate response of the levels to a field along z. The EPR transition occurs between the two lowest levels.

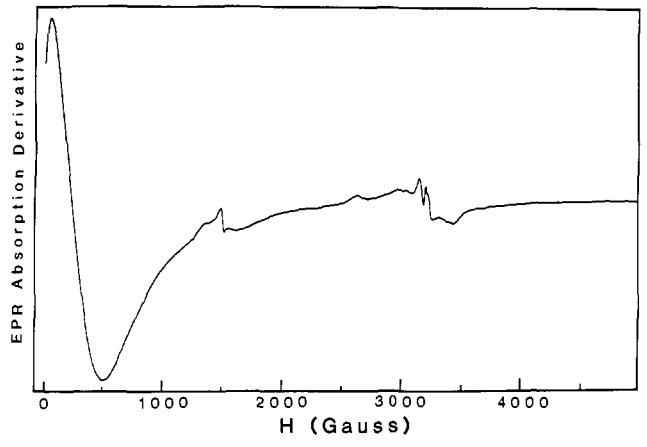

Figure 5. X-band EPR spectrum of a 2.2 mM sample of reduced Fd II (same sample as that of Figure 6). The low-field resonance is that indicated in Figure 4. The weak features at 1500 G are a minor (<1%) impurity, and the signal around 3300 G belongs to a $[Fe_4S_4]^{1+}$ cluster (<1% of total clusters in the sample). EPR conditions: $T = 9$ K; microwave frequency, 9.22 GHz; microwave power, 5 mW; modulation amplitude, 10 G.

by less than 0.4 cm^{-1}. Since the 0.06 T spectra are the same at 4.2 and 1.3 K, these must be the lowest levels. Second, the observation of magnetic interactions in weak applied fields shows that the electronic spin relaxation rate is slow on the Mössbauer time scale. Thus, the spectra need to be analyzed in the slow relaxation limit.

2. The spectrum of Figure 2 has a pattern typical of systems with uniaxial magnetic properties, i.e., for $H < 1.0$ T the electronic moment is appreciably different only for one direction. This implies $D < 0$ with either (a) $E/D \approx 0$ and D large or (b) $E/D > 0.2$ with $|D| \lesssim 5$ cm^{-1} (The range of E/D is $0 \leq E/D \leq 0.33$.). For case (b), a field of 6.0 T will mix excited states (essentially the $M = \pm 1$ sublevels) into the ground state whereas a large value of D will suppress such mixing. The 6.0 T spectrum clearly supports case (b). Thus, $0.20 < E/D < 0.33$ and $|D| < 5$ cm^{-1}. Figure 4 shows an energy level diagram pertinent to the $S = 2$ system of Fd II.

3. Our earlier preliminary studies indicated that the two lowest levels were separated by about 0.35 cm^{-1}. This suggested that one might be able to observe an EPR transition at X-band. Indeed we have observed at X-band at low field an extremely broad and weak signal (Figure 5) stretching virtually to zero magnetic field. This signal is absent in oxidized Fd II. A signal almost identical in shape was recently reported for the 3-Fe cluster of a ferredoxin from *Thermus thermophilus* and attributed to a "$\Delta m = 4$" transition.[30] The observation of such a signal down to zero field implies $\Delta \approx 0.30$ cm^{-1}. The splitting of the two states is given by $\Delta = 2D(x^{1/2} - 1)$ with $x = 1 + 3(E/D)^2$, putting constraints on the zero-field splitting parameters.

(30) Hagen, W. R.; Dunham, W. R.; Johnson, M. K.; Fee, J. A. *Biochim. Biophys. Acta* **1985**, *828*, 369–374.

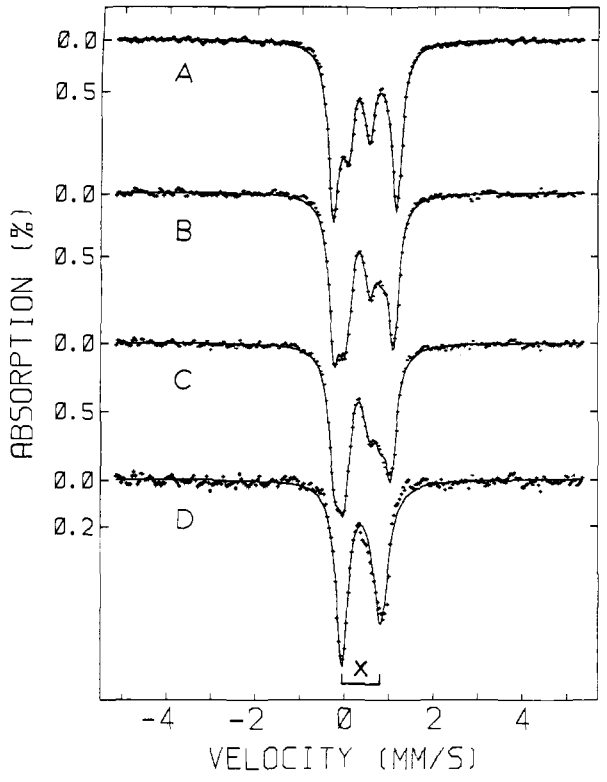

Figure 6. Mössbauer spectra of reduced Fd II, with ^{57}Fe in natural abundance, taken in zero-applied fields. Spectra were recorded at (A) 20, (B) 100, and (C) 150 K. The solid lines are least-squares fits as described in the text; parameters are given in Table II. The difference spectrum of (D), species X, was obtained by subtracting from the raw data (C) the 2:1 pattern of the ground-state configuration with use of the parameters of Table I.

4. At 1.3 K and for $H = 1.0$ T only the lowest electronic level is populated. For $E/D = 0.23$, our final choice, only the expectation value of the spin along z, $\langle S_z \rangle = -1.96$, is appreciably different from zero. Consequently, the internal field, $H_{int}(z) = -\langle S_z \rangle A_z/g_n\beta_n$, is along z, and A_z is measured. By studying the movement of the lines with increasing applied field, two spectral subcomponents are readily distinguished. One (≈33% of total Fe) shows increased magnetic splittings with increasing applied field. This component has therefore $A_z > 0$, and it corresponds to the "ferric" site II. The other component (≈67%) has $A_z < 0$. The movement of the absorption lines allows also assignments of the lines to each subcomponent.

5. All spectra can be explained as superpositions of just two components with occupation ratio 2:1. Despite the good resolution, we were unable to distinguish between the sites of the delocalized pair. Spectral simulations of the two subspectra are shown above the data of Figure 2.

6. The 1.0 T spectrum shows clearly that the ζ axes of the EFG tensors are tilted by an angle β relative to the z-axis of the electronic system. On the other hand, we found no evidence for rotation of the A tensors (which are quite isotropic anyway).

7. For applied fields $H > 1.0$ T level mixing becomes important. At $H \approx 2.0$ T the spectra become sensitive to A_x because $\langle S_x \rangle = -0.96$ is sizeable. At higher fields A_y can be determined.

8. In moderate applied fields, $0.2 \text{ T} < H < 0.6$ T, the expectation value $\langle S_z \rangle$ depends quite sensitively on E/D.

9. We have described the orientation of the EFG tensors relative to (x, y, z) by the Euler angles (α, β, γ). The spectra are not very sensitive to α and γ, and, therefore, we have chosen $\alpha = \gamma = 0$.

To summarize, ΔE_Q and δ are fixed by the zero-field spectra whereas A_z, η, and β are determined from the 1.0-T spectrum. In stronger fields, A_x and A_y become sensitive parameters. D and E/D are determined from the low-field spectra, the EPR data, and from the fits to the entire data set. In this way, the 16

Table II. Least-Squares Fitting Results of Zero-Field Spectra of Reduced Fd II[a]

T (K)	4.2	20	40	60	100	150	200
			Site I				
ΔE_Q (mm/s)	1.48	1.46	1.44	1.42	1.38	1.32	1.29
δ (mm/s)	0.46	0.46	0.45	0.45	0.44	0.41	0.39
Γ (mm/s)	0.28	0.29	0.29	0.28	0.27	0.27	0.26
			Site II				
ΔE_Q (mm/s)	0.47	0.48	0.48	0.48	0.49	0.51	0.49
δ (mm/s)	0.31	0.32	0.32	0.31	0.31	0.29	0.28
Γ (mm/s)	0.28	0.29	0.29	0.28	0.27	0.27	0.26
			Species X				
ΔE_Q (mm/s)		0.89	0.87	0.88	0.88	0.87	0.89
δ (mm/s)		0.39	0.39	0.40	0.39	0.38	0.36
Γ_L (mm/s)		0.26	0.27	0.29	0.29	0.33	0.30
Γ_R (mm/s)		0.70	0.50	0.48	0.43	0.44	0.40
%		7	16	22	30	45	55

[a] The fits were constrained as follows. The intensity ratio of sites I and II were fixed to 2:1. For both sites the width of the left lines, Γ_L, was set equal to that of the right line, Γ_R. For sites I and II the uncertainties in ΔE_Q, δ, and Γ are about ± 0.02 mm/s. The larger width, Γ_R, of species X may reflect inequivalencies of the three sites contributing to species X.

parameters listed in Table I were determined. The uncertainties were estimated from the final parameter set by varying individual parameters and comparing the simulated spectra by visual inspection.

High-Temperature Spectra. The spectra shown in Figure 6 were taken in zero applied field on a sample containing ^{57}Fe in natural abundance.[28] When the temperature is raised above 20 K the spectral resolution appears to decrease although the lines remain as sharp as observed at 4.2 K. Taking difference spectra (see Figure 6D) shows the appearance of a new doublet with $\Delta E_Q \approx 0.9$ mm/s and $\delta = 0.38$ mm/s. We have analyzed the spectra with least-squares fitting procedures by using two different sets of assumptions. First, we assumed that the two irons of site I become unequivalent as the temperature is raised. Thus, we fitted the spectra to three doublets with area ratio 1:1:1. This produced adequate fits by the χ^2 criterium. However, the widths Γ of the lines of the doublets were $\Gamma_1 \approx 0.36$, $\Gamma_2 \approx 0.23$, and $\Gamma_3 \approx 0.28$ mm/s for 20 K $< T <$ 210 K. The width Γ_3 of the ferric site is reasonable. However, Γ_2 is slightly below our instrumental width whereas Γ_1 is quite large. We find no plausible explanation why the width of one subsite of the cluster should be substantially larger than those of the other sites. More plausible fits were obtained by assuming that the spectra consist of the 2:1 pattern as observed at 4.2 K plus an additional doublet (species X). As shown in Table II, these assumptions resulted in reasonable and consistent parameters for the 2:1 pattern (sites I and II). For species X, we obtained values for ΔE_Q which were essentially independent of temperature. Two observations are of interest. First, the spectral 2:1 pattern converts into species X; at 200 K more than half of the absorption is contributed by the latter. Secondly, the isomer shift, $\delta \approx 0.39$ mm/s, of species X is fairly close to the weighted average of sites I and II. These observations suggest that species X represent a fully delocalized state where the excess electron is spread about equally over the three sites. Such a phenomenon has not yet been reported for an iron–sulfur cluster, but it is not without precedent in the inorganic literature. Only quite recently Mössbauer studies of oxo-centered trinuclear iron acetates $[Fe_3O(O_2CCH_3)_6(py)_3](py)$ in the mixed-valence state have demonstrated the appearance of a new doublet at higher temperatures. The new doublet was attributed to a localization–delocalization transition associated with an order–disorder transition in the crystalline state at $\sim$112 K.[31]

Spin-Coupling Model

In this section, we introduce a spin-coupling model for describing the low-temperature data of reduced Fd II. Three observations constitute the basis of the model. First, the data show clearly that the two irons of site I form a delocalized pair. Secondly, as judged by ΔE_Q and δ, site II (subsequently labeled site C) is high-spin ferric, with no evidence for delocalization. Thus, we will consider a model where site C is high-spin Fe^{3+} ($S_C = {}^5/_2$) and where the two irons of site I (subsequently labeled A and B) are indistinguishable and the excess electron is fully delocalized. Thirdly, by using a simple vector coupling model where S_C is antiferromagnetically coupled to the spin S_{AB} of the delocalized dimer, Münck and Kent[26] have argued that the observed value $A_C = +15.6$ MHz can be explained if $S_{AB} = {}^9/_2$. Since Fe_2S_2 dimers exhibit antiferromagnetic coupling and a ground-state spin $S_{AB} = {}^1/_2$ and since ferromagnetic contributions are expected to be much smaller than antiferromagnetic ones for Fe^{2+}/Fe^{3+} systems, the observation of a dimer spin $S_{AB} = {}^9/_2$ suggested a coupling model that had to include both Heisenberg exchange and a term describing valence delocalization.

We will test the model by computing the magnetic hyperfine interactions for sites A, B, and C from those reported for monomeric Fe^{3+} and Fe^{2+} with tetrahedral sulfur coordination. (The data of oxidized Fd II strongly suggest tetrahedral sulfur coordination for all sites). For the Fe^{3+} site, we can draw on data for rubredoxin, desulforedoxin, and Fe_2S_2 clusters and use $\bar{a}_{av}(Fe^{3+}) = -(20 \pm 2)$ MHz; the choice of this value is discussed in ref 11.

The choice of an appropriate value for Fe^{2+} sites is not immediately obvious. First, in contrast to the (almost) isotropic magnetic hyperfine interactions of Fe^{3+} sites, those of high-spin ferrous ions are considerably anisotropic because of sizable spin-dipolar and orbital contributions. By averaging the components, $a_{av} = (a_x + a_y + a_z)/3$, the spin-dipolar parts cancel. The orbital contributions can be estimated, in the framework of ligand field theory, from the known quadrupole and zero-field splitting parameters. However, since we do not have a good ligand field analysis for Fd II, we will not include such a correction and simply average the x, y, and z components, thus obtaining a values that include orbital contributions. For the uncoupled Fe^{2+} site we will use[32] $\bar{a}_{av}(Fe^{2+}) = -22.2$ MHz.

(31) (a) Oh, S. M.; Hendrickson, D. M.; Hassett, K. L.; Davis, R. E. *J. Am. Chem. Soc.* **1985**, *107*, 8009–8018. (b) Kambara, T.; Hendrickson, D. N.; Sorai, M.; Oh, S. M. *J. Chem. Phys.* **1986**, *85*, 2895–2909.

(32) Suitable reference compounds are reduced rubredoxin ($a_x = -27.4$ MHz, $a_y = -11.4$ MHz, $a_z = -31.5$ MHz, $a_{av} = -23.4$ MHz; ref 13a. The new value for $a_z = -31.5$ MHz is based on a recent data analysis which includes relaxation effects; it was communicated to us by P. G. Debrunner.), desulforedoxin ($a_x = a_y = -27.4$ MHz, $a_z = -9.2$ MHz, $a_{av} = -21.3$ MHz; ref 13b), and the tetrakisthiophenolate anion $Fe(SPh)_4$ ($a_x = -20.6$ MHz, $a_y = -11.2$ MHz, $a_z = -34.3$ MHz; $a_{av} = -22.0$ MHz; ref 13c). All three compounds are magnetically uniaxial at low temperature. Thus, while the data are quite sensitive to one component of the a tensor (a_y in rubredoxin and $Fe(SPh)_4$; a_z in desulforedoxin), the other two components were difficult to determine despite the sophisticated analyses employed, primarily because the zero-field splittings of these compounds are more than twice as large as those of Fd II. Rubredoxin and the synthetic complex have essentially the same values for a_y, ΔE_Q, η, and E/D; since D is 25% larger in rubredoxin, it is not clear to us whether the differences in a_x and a_z reflect uncertainties of the data analysis or structural differences. Although the structure of the desulforedoxin has not yet been determined, its Fe^{2+} site has $\Delta E_Q > 0$ like the delocalized pair of reduced Fd II and is thus attractive for comparison. Presently, it is perhaps best to average the a_{av} values of the three reference components, $\bar{a}_{av}(Fe^{2+}) = -22.2$ MHz.

In order to describe exchange interactions of localized spins and valence delocalization of one electron (or hole) we add a term to the Heisenberg Hamiltonian that mixes, for a dimer, the states $|S_A,S_B; S_{AB}\rangle^A$ and $|S_A,S_B; S_{AB}\rangle^B$. Here $|S_A,S_B; S_{AB}\rangle^A$ designates the ket of the coupled state $\vec{S}_A + \vec{S}_B = \vec{S}_{AB}$. (We will drop the magnetic quantum numbers.) The superscript A specifies that the excess electron resides on site A, e.g., for a Fe^{2+}/Fe^{3+} dimer site A is the ferrous site. We will describe the mixing by the term $B\hat{V}_{AB}\hat{T}_{AB}$ where $\hat{T}_{AB}$ is a transfer operator between site A and B and where the operator $\hat{V}_{AB}$ produces the factor $(S_{AB} + {}^1/_2)$ of Anderson and Hasegawa[19] and Borshch et al.[21] Thus, $\hat{V}_{AB}\hat{T}_{AB}|S_A,S_B; S_{AB}\rangle^B = \hat{V}_{AB}|S_A,S_B; S_{AB}\rangle^A = (S_{AB} + {}^1/_2)|S_A,S_B; S_{AB}\rangle^A$. The coefficient B is essentially a transfer integral. For a binuclear system we can write an effective Hamiltonian

$$\hat{\mathcal{H}} = [{}^AJ_{AB}{}^A\vec{S}_A\cdot{}^A\vec{S}_B + E_A]\hat{O}_A + [{}^BJ_{AB}{}^B\vec{S}_A\cdot{}^B\vec{S}_B + E_B]\hat{O}_B + B\hat{V}_{AB}\hat{T}_{AB} \quad (5)$$

The first two terms are the familiar Heisenberg Hamiltonian; ${}^AJ_{AB}$ is the exchange coupling constant between site A and B when the excess electron is on site A. Similarly, ${}^B\vec{S}_A$ is the spin operator of site A when the excess electron is on site B. $\hat{O}_A$ and $\hat{O}_B$ are occupation operators for sites A and B, respectively, defined by $\hat{O}_A|S_A,S_B; S_{AB}\rangle^A = |S_A,S_B; S_{AB}\rangle^A$ and $\hat{O}_B|S_A,S_B; S_{AB}\rangle^A = 0$, etc. E_A and E_B are the total energy of the system when the excess electron is on A or B.

For a symmetric dimer ($E_A = E_B$, ${}^AJ_{AB} = {}^BJ_{AB} = J$) eq 5 is readily solved in the subspace spanned by the kets $|S_A,S_B; S_{AB}\rangle^A$ and $|S_A,S_B; S_{AB}\rangle^B$, and we obtain the known[21] result

$$E = \frac{J}{2}S_{AB}(S_{AB} + 1) \pm B(S_{AB} + {}^1/_2) \quad (6)$$

A more extensive discussion of the dimer system including treatments of electronic Zeeman terms and magnetic hyperfine terms will be given elsewhere.[33]

For the description of trinuclear and tetranuclear clusters, we will generalize eq 5 and propose the following effective Hamiltonian

$$\hat{\mathcal{H}} = \sum_k[\sum_{i<j}{}^kJ_{ij}{}^k\vec{S}_i\cdot{}^k\vec{S}_j + E_k]\hat{O}_k + \sum_{n<m}B_{nm}\hat{V}_{nm}\hat{T}_{nm} \quad (7)$$

where k sums over the sites which can be occupied by the itinerant electron. The transfer term in eq 7 is more based on intuition than on a derivation from microscopic theory. For a few simple cases, we have compared the energy levels obtained from microscopic theory with those obtained from eq 7. These simple cases include binuclear systems with n electrons on A and $(n + 1)$ electrons on B and a trinuclear system with three localized and one itinerant electron.

For the description of trimers with a delocalized pair AB we choose the basis states $|S_AS_B(S_{AB}), S_C; S\rangle^i$ where S is the total spin and S_{AB} an intermediate spin, $\vec{S}_{AB} = \vec{S}_A + \vec{S}_B$, and i = A, B. The occupation and transfer operators are defined[34] such that

$$\hat{O}_k|S_AS_B(S_{AB}), S_C; S\rangle^i = \delta_{ik}|S_AS_B(S_{AB}), S_C; S\rangle^i \quad (8)$$

$$\hat{T}_{AB}|S_AS_B(S_{AB}), S_C; S\rangle^B = |S_AS_B(S_{AB}), S_C; S\rangle^A \quad (9)$$

$$\hat{V}_{AB}|S_AS_B(S_{AB}), S_C; S\rangle^i = (S_{AB} + {}^1/_2)|S_AS_B(S_{AB}), S_C; S\rangle^i \quad (10)$$

In these expressions i = A, B and k = A, B. For the computation of $\hat{V}_{AB}|S_A, S_BS_C(S_{BC}); S\rangle^i$ or $\hat{T}_{AB}|S_A, S_BS_C(S_{BC}); S\rangle^i$ one can expand $|S_A, S_BS_C(S_{BC}); S\rangle^i$ in the basis $|S_AS_B(S_{AB}), S_C; S\rangle^i$ where the expansion coefficients can be expressed by 6-j symbols.

For Fd II, we apply eq 7 with the following assumptions. AB will be the only delocalized pair; $B_{AB} = B$, $B_{AC} = B_{BC} = 0$. In order to make A and B equivalent, we choose $E_A = E_B$. Further, we will assume that all exchange coupling constants J are equal.[35]

With these assumptions, eq 7 can be written as

$$\hat{\mathcal{H}} = J[{}^A\vec{S}_A\cdot{}^A\vec{S}_B + ({}^A\vec{S}_A + {}^A\vec{S}_B)\cdot\vec{S}_C]\hat{O}_A + J[{}^B\vec{S}_A\cdot{}^B\vec{S}_B + ({}^B\vec{S}_A + {}^B\vec{S}_B)\cdot\vec{S}_C]\hat{O}_B + B\hat{V}_{AB}\hat{T}_{AB} \quad (11)$$

The terms in brackets are diagonal in the basis $|S_AS_B(S_{AB}), S_C; S\rangle^A$, $|S_AS_B(S_{AB}), S_C; S\rangle^B$ with $S_{AB} = {}^1/_2, {}^3/_2, \cdots {}^9/_2$ and $|S_{AB} - {}^5/_2| \le S \le |S_{AB} + {}^5/_2|$. The transfer term mixes only states with the same S and S_{AB}, and thus the eigenvalues of eq 11 are simply

$$E = \frac{J}{2}S(S + 1) \pm B(S_{AB} + {}^1/_2) \quad (12)$$

with eigenvectors ($|S_AS_B(S_{AB}), S_C; S\rangle \equiv |S_{AB}; S\rangle$)

$$|S_{AB}; S\rangle_\pm = \frac{1}{2^{1/2}}(|S_{AB}; S\rangle^A \pm |S_{AB}; S\rangle^B) \quad (13)$$

In Figure 7, we have plotted the energies of the lowest levels ($S = 0, 1, 2$ for $J > 0$) vs. B/J. For $B/J = 0$ each state with a given S and S_{AB} occurs twice ($|S_{AB}; S\rangle^A$ and $|S_{AB}; S\rangle^B$). If delocalization is allowed, these states mix and split by $\pm B(S_{AB} + {}^1/_2)$. For small B/J, the ground state has $S = 0$. The system assumes the $|{}^9/_2; 2\rangle_-$ ground state for $|B|/J > 2$. We will compute the hyperfine coupling constants A of the coupled system by equating the expectation values of

$$A_AS_z = {}^Aa_A{}^AS_{Az}\hat{O}_A + {}^Ba_A{}^BS_{Az}\hat{O}_B \quad (14)$$

$$A_BS_z = {}^Aa_B{}^AS_{Bz}\hat{O}_A + {}^Ba_B{}^BS_{Bz}\hat{O}_B$$

$$A_CS_z = a_CS_{Cz}$$

for the $|{}^9/_2; 2\rangle_-$ ground state. A straightforward calculation[36] yields

$$A_A = A_B = \frac{11}{108}(4{}^Aa_A + 5{}^Ba_A) \quad (15)$$

$$\text{and} \qquad A_C = -({}^5/_6)a_C$$

In eq 15 ${}^Aa_A$ is the a value of site A when the excess electron is on A, i.e., ${}^Aa_A$ describes a ferrous site; thus we set ${}^Aa_A = {}^Ba_B = \bar{a}_{av}(Fe^{2+}) = -22.2$ MHz and ${}^Aa_B = {}^Ba_A = a_C = \bar{a}_{av}(Fe^{3+}) = -20$ MHz. Substituting these values into eq 15 yields $A_A = A_B = -19.2$ MHz and $A_C = +16.7$ MHz. Thus, the signs and magnitude are in very good agreement with the experimental values $A_I = A_A = A_B = -19.1$ MHz and $A_{II} = A_C = +15.6$ MHz. The state $|S_{AB}; S\rangle_- = |{}^7/_2; 2\rangle_-$ produces $A_A = A_B = -7.5$ MHz and $A_C = +1.7$ MHz. All other states with $S_{AB} < {}^7/_2$ not only yield poor numerical values but also the wrong sign for A_C.

In order to produce a ground state with $S = 2$ and $S_{AB} = {}^9/_2$, the coupling constant J must be positive (antiferromagnetic coupling). The sign of B remains undetermined because both the symmetric and antisymmetric states of eq 13 produce the same A values.

We have made above the assumption that site A and B are equivalent. If we relax this condition, the eigenstates take the form

$$|S_{AB}; S\rangle = \cos\alpha|S_{AB}; S\rangle^A + \sin\alpha|S_{AB}; S\rangle^B$$

where α is a mixing parameter. While α affects A_A and A_B, the value for A_C is independent of α. This is, of course, a consequence of the fact tht S_{AB} is a good quantum number. These considerations justify the simple vector coupling model used by Münck and Kent[26] for the determination of $S_{AB} = {}^9/_2$.

In principle, one can use solution (13) to compute the zero-field splitting of the cluster by using the parameters of the mononuclear reference compounds. However, since the relative orientations of the tensors are not known, the number of unknowns by far

(33) Blondin, G.; Charlot, M. S.; Girerd, J.-J., manuscript in preparation.

(34) For the simple case of one delocalized pair the two Hermetian operators $\hat{V}_{km}$ and $\hat{T}_{km}$ can be combined. For more complex cases such as tetranuclear clusters it is convenient to use separate operators.

(35) One would expect that ${}^AJ_{AC} = {}^BJ_{BC} = J'$ and ${}^BJ_{AC} = {}^AJ_{BC} = J''$ and ${}^AJ_{AB} = {}^BJ_{AB} = J'''$. For $J' = J'' \neq J'''$, we obtain the same eigenfunctions and thus the same A values as given in the text.

(36) For the evaluation of the matrix elements, one has to keep in mind that $|S_A, S_B; S_{AB}\rangle^A = |2, {}^5/_2; {}^9/_2\rangle$ while $|S_A, S_B; S_{AB}\rangle^B = |{}^5/_2, 2; {}^9/_2\rangle$, i.e., the site with the extra electron is high-spin ferrous; ${}^AS_A = {}^BS_B = 2$, ${}^BS_A = {}^AS_B = {}^5/_2$.

exceeds the information available. Nevertheless, by keeping all tensors in the same frame our calculations suggest that one needs $D < 0$ for the Fe^{2+} site. Thus, ferrous desulforedoxin ($D = -6$ cm^{-1}, ref 13c) seems to be more suitable than rubredoxin ($D = +7.9$ cm^{-1}, ref 13a) or the $Fe(SPh)_4$ anion ($D = +6.2$ cm^{-1}, ref 13b). Interestingly, desulforedoxin has also $\Delta E_Q > 0$, just as the delocalized pair of Fd II. Finally, Table I shows that $\tilde{A}_1$ is remarkably isotropic. Since ferric and ferrous a values are averaged according to eq 15, we expect that the anisotropies are reduced roughly by a factor 2. Other effects, however, are likely to contribute to this reduction as well.[37] One should keep in mind, however, that the structure of the Fd II cluster is not known and that, therefore, none of the reference compounds used may be suitable to explain these finer points.

Discussion

In the preceding sections, we have described in some detail the analysis of the Mössbauer spectra of reduced Fd II. Because of the peculiar nature of the electronic system the spectra taken in strong applied fields are extremely well resolved. By studying the sample under different experimental conditions it was possible to determine subsets of the parameters independently and thus determine 16 electronic and hyperfine parameters with good precision.

As pointed out previously,[2] the cluster is a mixed valence system exhibiting both a localized site and a delocalized pair. Even with the excellent resolution of the low-temperature Mössbauer spectra no differences between sites A and B of the pair could be discerned. It is also noteworthy that the spin Hamiltonian of eq 1–4 fits the whole low-temperature data set quite well, suggesting that the spin quintet is well isolated and that excited states capable of mixing with the quintet in a 6.0-T field are separated by at least 20 cm^{-1} from the ground manifold.

We have introduced here a model Hamiltonian which takes both Heisenberg exchange and valence delocalization into account. To our knowledge this is the first time that such a Hamiltonian has been used to describe the magnetic properties of a mixed-valence system. Two observations suggested the particular model employed. First, the quadrupole splittings and isomer shifts of sites A and B are identical (as are the magnetic interactions) and indicative of iron at the $Fe^{2.5+}$ oxidation level; site C is clearly Fe^{3+}. Second, the considerations of Münck and Kent[26] lead to the recognition that the spin of the internally delocalized dimer is $S_{AB} = {}^9/_2$. Since very similar magnetic patterns have been observed for all Fe_3S_4 clusters studied, and since for Fe^{2+}/Fe^{3+} systems ferromagnetic contributions to the exchange coupling are expected to be much smaller than antiferromagnetic contributions, a different coupling mechanism was indicated for the dimer. Noodleman and Baerends,[20] applying LCAO-Xα valence bond theory to Fe_2S_2 clusters, have suggested that valence delocalization in the mixed valence state can give rise to a resonance splitting proportional to $B(S_{AB} + {}^1/_2)$, where B is essentially a transfer integral. Similar suggestions were put forward by Belinskii, Tsukerblat, and Gerbeleu[22b] and Borshch, Kotov, and Bersuker.[21] The expression for the resonance splitting is the same as that proposed by Anderson and Hasegawa[19] in their fundamental paper on double exchange.

While the perceptive theoretical analysis of Noodleman and Baerends refers to Fe_2S_2 clusters with known (or assumed) structure, our aim is to describe experimental data of clusters of unknown structure by an effective coupling Hamiltonian.

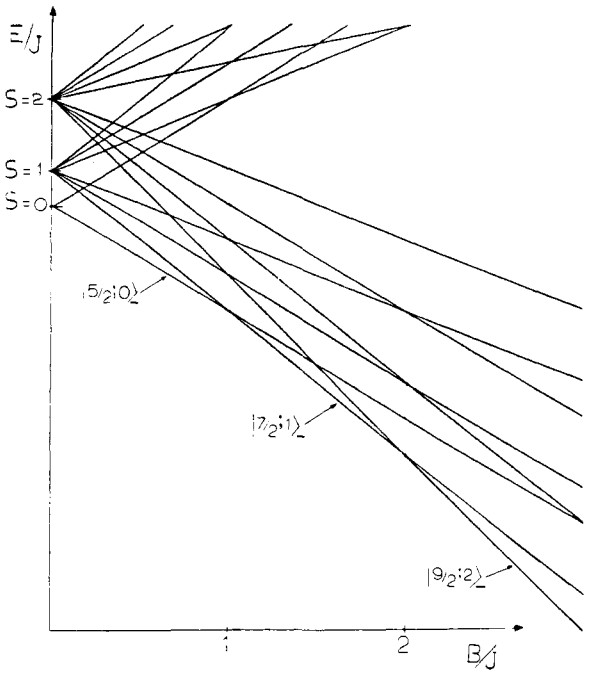

Figure 7. Energy level scheme according to eq 12, shown for the states with system spins $S = 0$, 1, and 2. Emphasis is on the lowest energy levels.

Therefore, we have amended the usually employed Heisenberg Hamiltonian by a term describing the delocalization of *one* electron within a subdimer of the 3-Fe cluster. This was achieved by adding the transfer term in eq 7. We kept the model as simple as possible. Thus, we have assumed that the three coupling constants J_{ij} are the same, $J_{ij} = J$. We have also neglected vibronic interactions (which lead to a non-Heisenberg behavior[22,23]). By using data from studies of mononuclear Fe^{3+} and Fe^{2+} complexes, our model reproduces the experimental A values remarkably well. Both signs and magnitudes are predicted well by the theory. In fact, the uncertainties in $\bar{a}_{av}(Fe^{3+})$ and $\bar{a}_{av}(Fe^{2+})$ are certainly larger than the deviations between theory and experiment.

Although the magnitudes of J and B are still unknown for reduced Fd II, the energy level diagram of Figure 7 contains some interesting information. It can be seen that the spin of the cluster ground state depends quite sensitively on B/J. For $J > 0$ (antiferromagnetic coupling) and $B/J > 2$ we obtain the ground state of Fd II with $S = 2$ and $S_{AB} = {}^9/_2$. The sign of B remains undetermined. Recently, Rusnak et al.[38] described a novel 3-Fe cluster for a hydrogenase from *Clostridium pasteurianium*. In the reduced state, this cluster exhibits a quadrupole doublet pattern exactly like that of Fd II. Yet, the cluster has an electronic ground state with $S = 0$. Our model predicts such a solution for $J > 0$ and $B/J < 1$.

All $[Fe_2S_2]^{1+}$ dimers studied thus far have a ground state with $S = {}^1/_2$ and localized valence states. The oxidized $[Fe_2S_2]^{2+}$ clusters ($S = 0$) have $J > 150$ cm^{-1}. EPR studies[39] of *oxidized* Fd II suggest $J \approx 20$ cm^{-1}; this is in agreement with our Mössbauer studies.[37] Thus it appears that 3-Fe clusters may more easily achieve large B/J ratios and thus a large dimer spin.

It would be interesting to test the energy level scheme of Figure 7 by techniques such as magnetic susceptibility. However, our Mössbauer studies at $T > 20$ K suggest that an additional low-lying state other than those of Figure 7 need to be considered. The Mössbauer spectra suggest that a new doublet, reflecting a fully delocalized state, appears at $T > 20$ K. Since our coupling model assumes one Fe^{3+} site and one delocalized pair, the state yielding new doublet is not represented in Figure 7. We do not

(37) Although the a tensors of ferric rubredoxin[13a] and desulforedoxin[13c] are isotropic to within 5%, the components of the a tensors of the Fe^{3+} sites of $[Fe_2S_4]^{1+}$ clusters deviate by as much as ±15% from a_{av}.[15b,16] Recently, a refined analysis of the Mössbauer spectra of oxidized Fd II revealed large anisotropies of the Fe^{3+} sites. This anisotropy is caused by mixing of electronic states by the zero-field splitting terms for $D/J \approx 0.1$ (for Fe^{3+}-rubredoxin,[13a] $D = 1.9$ cm^{-1}): Papaefthymiou, V.; Münck, E.; Moura, I.; Moura, J. J. G., manuscript in preparation. In principle one would have to add the zero-field splittings of the uncoupled ions to the Hamiltonian of eq 7. However, since we have no evidence that such terms are required for the description of reduced Fd II and since such terms would add a large number of unknowns, we have not considered these terms here. The incorporation of such terms into the present formalism will be discussed in ref 33 for binuclear centers.

(38) Rusnak, F.; Adams, M. W. W.; Mortenson, L. E.; Münck, E. *J. Biol. Chem.* **1987**, *262*, 38–41.

(39) Guigliarelli, B.; Gayda, J. P.; Bertrand, P.; More, C. *Biochim. Biophys. Acta* **1986**, *871*, 149–155.

yet understand the nature of the postulated excited state. It is interesting to note that the transition rate between the ground-state manifold and the excited-state configuration is slow on the time scale of Mössbauer spectroscopy ($\sim 10^{-7}$ s). Such a phenomenon has not yet been reported for iron–sulfur clusters. Interestingly, Borshch et al.[40] have published a theoretical study of electron delocalization in trinuclear mixed valence clusters taking into account vibronic interactions. These authors point out that localized and delocalized states can co-exist in certain temperature ranges and that such states may be observable by Mössbauer spectroscopy.

We have little information on the magnetic properties of the postulated excited state. The Hamiltonian of eq 7 is flexible enough to describe the fully delocalized configuration. This could be accomplished by adding delocalization between sites A and C and sites B and C. On the other hand, it is quite likely that a more comprehensible description requires some consideration of vibronic coupling.

The coupling Hamiltonian of eq 7 can be adapted to describe tetranuclear clusters. We are currently analyzing data of Fe_4S_4 and $CoFe_3S_4$ clusters, and the initial results are promising.

Acknowledgment. We thank Dr. J. LeGall for providing us generously with ^{57}Fe enriched *D. gigas* cells. We are grateful to Dr. O. Kahn, who suggested that the concept of double exchange may be applicable to Fd II. This work was supported by the National Science Foundation, the National Institutes of Health, the Instituto de Investigacão Cientifica Tecnologica, the Junta National de Investigacão Cientifica Tecnologica, and by a NATO Collaborative Research (RG86/0099) grant.

Registry No. Fe, 7439-89-6; S, 7704-34-9.

(40) Borshch, S. A.; Kotov, I. N.; Bersuker, I. B. *Chem. Phys. Lett.* **1982**, *89*, 381–384.

Communications to the Editor

Allylcerium(III) Compounds, Powerful New Synthetic Reagents. A New Stereocontrolled Approach to Olefins and Methylene-Interrupted Polyenes

Bao-Shan Guo, Wendel Doubleday, and Theodore Cohen*

Department of Chemistry, University of Pittsburgh Pittsburgh, Pennsylvania 15260

Received February 25, 1987

We have recently reported that reductive metalation of allyl phenyl sulfides is a versatile and general preparative method for hydrocarbon allyl anions and that the latter, in the presence of titanium tetraisopropoxide, add in a 1,2-fashion to enals only *at the most substituted terminus of the allyl system.*[1,2] We now reveal simple procedures for securing 1,2-addition to aldehydes and enals mainly *at the least substituted terminus of such allyl anions*, a unique outcome[3] which results in *either cis or trans homoallylic alcohols with high stereocontrol.*

σ-Bonding between allyl and metal ions apparently occurs at the least hindered allyl terminus, and the metal behaves as a Lewis acid toward the carbonyl oxygen atom, thus positioning the carbonyl carbon atom for attack at the most substituted terminus.[1,2] In order to induce attack at the least sterically hindered terminus, we sought a metal which is unlikely to form a σ-bond to the allyl anion and yet which strongly complexes oxygen so as to encourage 1,2- rather than 1,4-addition to enals and enones.[4] Since certain allyllanthanides apparently involve trihapto bonding,[5] we examined cerium(III),[6] which had been found by Imamoto[7] to be highly oxophilic toward the carbonyl group and to cause 1,2-addition of an anion to an enal. Treatment of the lithium salt

Table I.

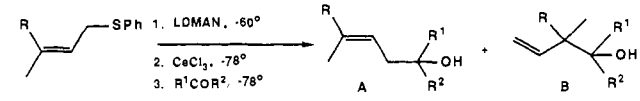

R	R^1	R^2	% yield A[a]	% yield B[a]
CH_3	Ph	H	53	12
CH_3	*trans*-CH_3CH=CH	H	73	14
CH_3	$(CH_3)_2C$=CH	CH_3	58	34
CH_3	$(CH_2)_5$		45	16
CH_3	CH=$CH(CH_2)_3$		47	40
CH_3	*trans*-PhCH=CH	H	56	24
H	Ph	H	47	13
H	CH_2=CH	H	53	13
H	*trans*-CH_3CH=CH	H	59	25
H	*trans*-PhCH=CH	H	42	25
H	$(CH_2)_5$		48	35

[a] Isolated, nonoptimized yields.

Scheme I

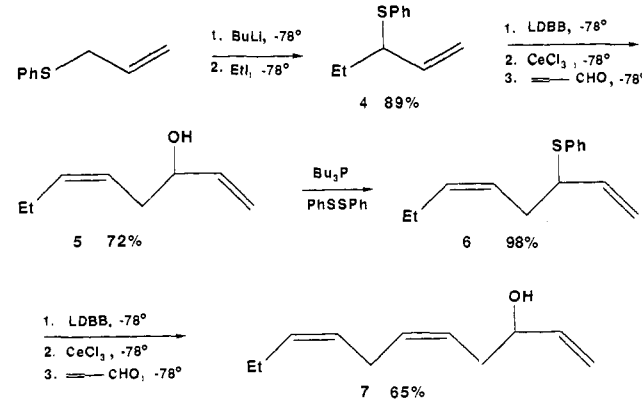

(1) Cohen, T.; Guo, B.-S. *Tetrahedron* **1986**, *42*, 2803.

(2) Other recent work with allyltitaniums: Reetz, M. T.; Steinbach, R.; Westermann, J.; Peter, R.; Wenderoth, B. *Chem. Ber.* **1985**, *118*, 1441.

(3) Okude, Y.; Hirano, S.; Hiyama, T.; Nozaki, H. *J. Am. Chem. Soc.* **1977**, *99*, 3179 and note 4 therein.

(4) Lefour, J.-M.; Loupy, A. *Tetrahedron* **1978**, *34*, 2597. Wartski, L.; El Bouz, M. *Tetrahedron* **1982**, *38*, 3285 and references therein.

(5) Tsutsui, M.; Ely, N. *J. Am. Chem. Soc.* **1975**, *97*, 3551. See also: Hodgson, K.; Mares, F.; Starks, D.; Streitwieser, A., Jr. *Ibid.* **1973**, *95*, 8650.

(6) Reviews of organolanthanides: Marks, T. J.; Ernst, R. D. In *Comprehensive Organometallic Chemistry*; Wilkinson, G., Stone, F. G. A., Abel, E. W., Eds.; Pergamon: Oxford, 1982; Chapter 21. Schumann, H. *Angew. Chem., Int. Ed. Engl.* **1984**, *23*, 474. Natale, N. R. *Org. Prep. Proced. Int.* **1983**, *15*, 389. Kagan, H. B.; Namy, J. L. *Tetrahedron* **1986**, *42*, 6573.

(7) Imamoto, T.; Sugiura, T.; Takiyama, N. *Tetrahedron Lett.* **1984**, *25*, 4233. Imamoto, T.; Kusumoto, T.; Tawarayama, T.; Sugiura, Y.; Mita, T.; Hatanaka, Y.; Yokoyama, M. *J. Org. Chem.* **1984**, *49*, 3904. After our discovery of the generality of the 1,2-addition of allylceriums to enals and enones, papers by Imamoto appeared indicating the generality of 1,2-additions of organocerium(III) compounds to enones: Imamoto, T.; Sugiura, Y. *J. Organomet. Chem.* **1985**, *285*, C21. Imamoto, T.; Takiyama, N.; Nakamura, K. *Tetrahedron Lett.* **1985**, *26*, 4763.

0002-7863/87/1509-4710$01.50/0